Earth and Planetary Science Letters 381 (2013) 166–176

Contents lists available at ScienceDirect

Earth and Planetary Science Letters

www.elsevier.com/locate/epsl

The extent of continental crust beneath the Seychelles

J.O.S. Hammond [a,*], J.-M. Kendall [b], J.S. Collier [a], G. Rümpker [c]

[a] Dept. of Earth Science and Engineering, Imperial College London, Exhibition Road, London, SW7 2AZ, UK
[b] School of Earth Sciences, University of Bristol, Wills Memorial Building, Queens Road, Bristol, BS8 1RJ, UK
[c] Institute of Geosciences, Goethe-University Frankfurt, Altenhoeferallee 1, 60438 Frankfurt/Main, Germany

ARTICLE INFO

Article history:
Received 13 April 2013
Received in revised form 1 August 2013
Accepted 11 August 2013
Available online 25 September 2013
Editor: P. Shearer

Keywords:
receiver functions
gravity
crustal structure
microcontinent

ABSTRACT

The granitic islands of the Seychelles Plateau have long been recognised to overlie continental crust, isolated from Madagascar and India during the formation of the Indian Ocean. However, to date the extent of continental crust beneath the Seychelles region remains unknown. This is particularly true beneath the Mascarene Basin between the Seychelles Plateau and Madagascar and beneath the Amirante Arc. Constraining the size and shape of the Seychelles continental fragment is needed for accurate plate reconstructions of the breakup of Gondwana and has implications for the processes of continental breakup in general. Here we present new estimates of crustal thickness and V_P/V_S from H–κ stacking of receiver functions from a year long deployment of seismic stations across the Seychelles covering the topographic plateau, the Amirante Ridge and the northern Mascarene Basin. These results, combined with gravity modelling of historical ship track data, confirm that continental crust is present beneath the Seychelles Plateau. This is $\sim$ 30–33 km thick, but with a relatively high velocity lower crustal layer. This layer thins southwards from $\sim$ 10 km to $\sim$ 1 km over a distance of $\sim$ 50 km, which is consistent with the Seychelles being at the edge of the Deccan plume prior to its separation from India. In contrast, the majority of the Seychelles Islands away from the topographic plateau show no direct evidence for continental crust. The exception to this is the island of Desroche on the northern Amirante Ridge, where thicker low density crust, consistent with a block of continental material is present. We suggest that the northern Amirantes are likely continental in nature and that small fragments of continental material are a common feature of plume affected continental breakup.

1. Introduction

Small slivers of continental crust, or 'microcontinents' are found in most of the Earth's oceans. Their identification is relatively straight-forward, differing from typical oceanic crust by having thicker crust, lower seismic velocities and lacking seafloor-spreading magnetic lineations (Carlson et al., 1980; Nur and Ben-Avraham, 1982). One of the best examples of a microcontinent is the Seychelles Plateau with its series of granitic islands, located in the Indian Ocean. These spectacular granitic outcrops were first noted as unusual by Darwin (1839) and later cited by Wegener (1924) as evidence for continental drift. Additionally, recent studies have shown that the Indian Ocean may contain many small fragments of continental crust isolated during the complex breakup of Madagascar–Seychelles–India (Minshull et al., 2008; Torsvik et al., 2013). In this study we present estimates of crustal thickness and the ratio of V_P to V_S derived from receiver functions across the Seychelles covering the topographic plateau, the Amirante Ridge and the northern Mascarene Basin. These results combined with an analysis of gravity data, show for the first time the extent of continental crust in this region.

2. The Seychelles microcontinent

The Seychelles are made up of 115 islands, the majority of which are small coral atolls, but 41 have a granitic composition, and are found around the main islands of Mahé and Praslin (Fig. 1). The granites are similar petrologically, geochemically and in age to the granites found on Madagascar and north–west India, and were likely formed in an Andean arc-like setting $\sim$ 750 Ma (Tucker et al., 2001; Ashwal et al., 2002). The Seychelles granites are thought to have been emplaced in two main stages, with the grey granites of Mahé being slightly older than the pink Praslin granites (Weis and Deutsch, 1984). The Seychelles granites are cut by numerous doleritic dykes with predominantly WNW–ESE trends which were emplaced in two stages, one in the Precambrian and

* Corresponding author.
E-mail address: j.hammond@imperial.ac.uk (J.O.S. Hammond).

0012-821X © 2013 The Authors. Published by Elsevier B.V. Open access under CC BY license.
http://dx.doi.org/10.1016/j.epsl.2013.08.023

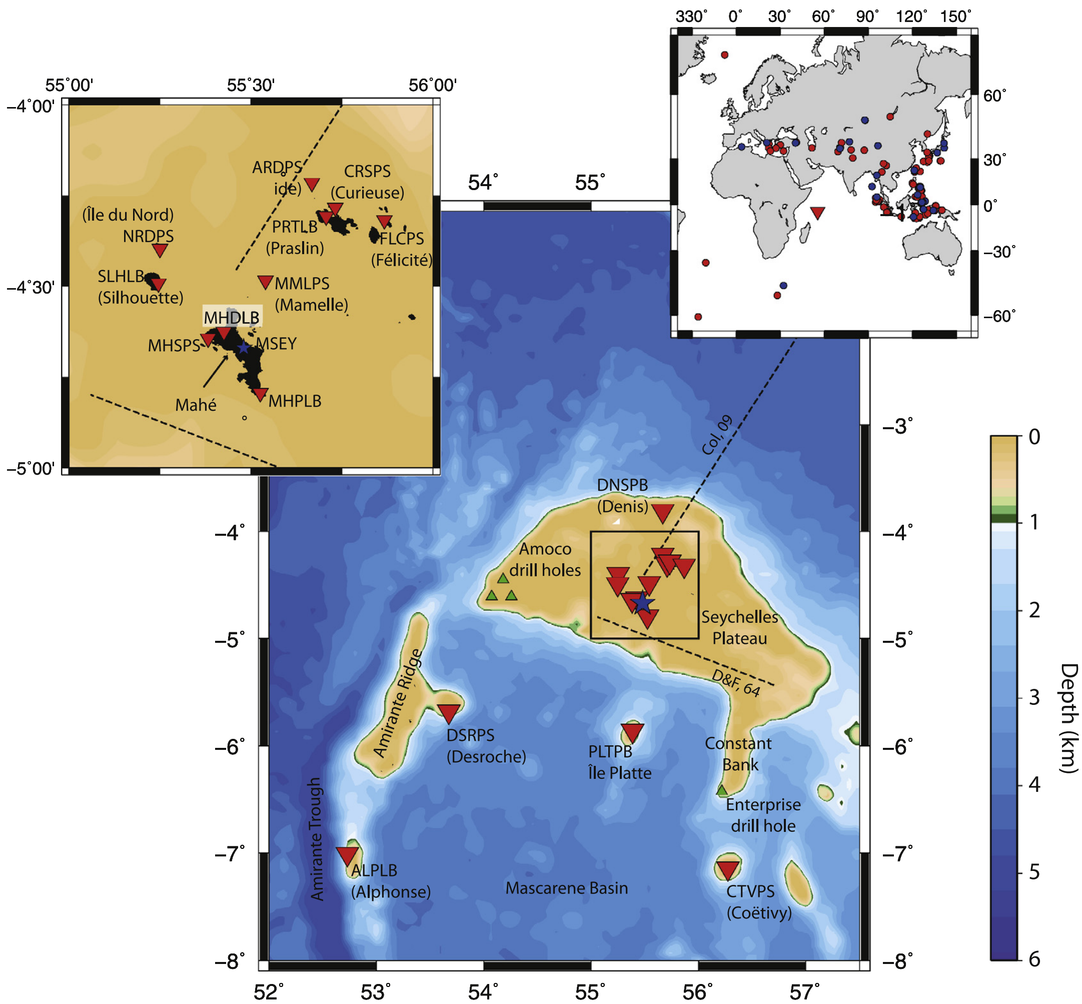

Fig. 1. Seismic stations used in the study. Inverted red triangles show seismic stations in our array, the blue star shows the permanent station MSEY, the dashed line shows the controlled source profile of Davies and Francis (1964) (D&F, 64) and Collier et al. (2009) (Col, 09). Also shown are the seismic events used in this study (top right) where red dots show events used at MSEY and blue dots show those used at the temporary seismic array. The inverted triangle shows the approximate location of the Seychelles. (For interpretation of the references to color in this figure legend, the reader is referred to the web version of this article.)

one in the early Tertiary (Suwa et al., 1994). Other volcanics are found on the Seychelles, most spectacularly in the form of the islands of Silhouette and Île du Nord. These islands form alkaline igneous complexes, dated to 61–67 Ma (Dickin et al., 1986; Ganerod et al., 2011), similar in age to the second emplacement of doleritic dykes and likely linked with the Deccan Trap formation, when the Seychelles is thought to be positioned proximal to India (Collier et al., 2008).

Early refraction work determined the crustal thickness beneath the central part of the plateau to be 33 km with a typically continental velocity profile in the crust (Gaskell et al., 1958; Shor and Pollard, 1963; Davies and Francis, 1964; Francis et al., 1966; Francis and Shor, 1966; Matthews and Davies, 1966). More recent controlled source seismic data provide good constraints on the northernmost extent of continental crust beneath the Seychelles (Collier et al., 2009). Further constraints exist from hydrocarbon exploration during the 1980's when Amoco drilled three holes on the southwesternmost extent of the topographic plateau (Fig. 1). Drilling encountered Triassic/Jurassic sediments and showed evidence of hydrocarbons suggesting continental crust extends to the southwesternmost tip of the topographic plateau (Coakley, 1997; Franks et al., 2006). In the mid 1990's Enterprise also drilled a hole on Constant Bank, but this encountered thick volcanics and the crustal affinity remained unclear. Despite this work, the southern margin, including the nature of the crust beneath the enigmatic Amirante Ridge and the northern Mascarene Basin remains poorly known.

3. Data

A major onshore–offshore controlled source experiment was conducted in February 2003 to constrain the north Seychelles passive margin (Collier et al., 2009). This involved the deployment of 32 ocean bottom seismometers, 8 broadband and 18 short-period, three component seismometers on islands throughout the Seychelles. Following the controlled source experiment the land based stations were relocated to cover a broad region of the Seychelles microcontinent and were left recording for one year (see Hammond et al., 2005; Collier et al., 2009, for details). The majority of the stations were located on the granitic islands of Mahé and Praslin and their satellite islands. More distant sites were situated on coral islands on the northern edge of the Seychelles Plateau and along the Amirante Ridge and Mascarene Basin. Additionally this study uses data from a permanent seismic station (MSEY) on Mahé, the largest of the Seychelles islands (Fig. 1). The aperture of the resulting roughly triangular array was on the order of 500 km (Fig. 1).

During the period of deployment 239 earthquakes > 5.8 Mb were recorded, of which 101 fell in to a suitable range for generating receiver functions (RF) (40°–90°).

4. Receiver functions

The receiver function method is a useful tool for determining the structure beneath a seismic station. It works on the principle that the coda which follows a P-wave teleseismic arrival is primarily made up of P-to-S-wave converted phases and their multiples generated by impedance contrasts at interfaces near the receiver. As a result a convolution of the incident wave with Earth structure is recorded at the seismometer. It is possible to estimate Earth structure by deconvolving the incident wave (P-wave on the vertical component) from the radial component. This produces a series of spikes on the radial component called the receiver function.

The main challenge in generating these receiver functions is the process of deconvolution. Deconvolution can become unstable in the presence of noise (Gurrola et al., 1995). As a result, many methods of deconvolution have been implemented when generating receiver functions, including, division in the frequency domain (Langston, 1979; Owens et al., 1984; Ammon, 1991), application of damped least squares in the time domain (Oldenburg, 1981; Abers et al., 1995), iteratively deconvolving in the time domain (Gurrola et al., 1995; Ligorria and Ammon, 1999) and multi-taper frequency domain cross-correlation (MTRF) (Park and Levin, 2000; Helffrich, 2006).

The method used in this study is the extended-time multi-taper receiver function method (ETMTRF) (Helffrich, 2006) which is based on the multi-taper receiver function (MTRF) method of Park and Levin (2000). For this study the ETMTRF method is ideal due to its behaviour in the presence of noise, as stations located on small islands record high levels of noise in the same frequency band as teleseismic signals. The ETMTRF method calculates the frequency spectrum using leakage resistant multi-tapers which are damped depending on the pre-event noise spectrum. This means low-amplitude regions of the P-wave spectrum can be used in the RF estimate enabling high frequency, high resolution RFs to be generated (see Helffrich, 2006, for details). In this study all receiver functions have a frequency domain low-pass $\cos^2$ taper with a 1.5 Hz cut-off applied to them.

4.1. H–κ stacking method

It is possible to invert RFs for the velocity and depths of subsurface layers. However, without the inclusion of an a priori velocity model it is hard to account for the non-uniqueness inherent in determining the depths of discontinuities highlighted in the RF (Ammon et al., 1990). One way to reduce this ambiguity is to use multiples of direct arrivals to place constraints on H (depth) and κ (V_P/V_S) (Zandt and Ammon, 1995). This study follows methods outlined in Zhu and Kanamori (2000). By using the converted phase from the Moho, *Ps*, and its crustal multiples, *PpPs* and *PpSs* + *PsPs*, it is possible to stack the RFs in the H–κ domain using

$$s(H,\kappa) = r(t_1) + r(t_2) + r(t_3), \tag{1}$$

where $r(t_i)$ is the amplitude of the radial RF for the predicted arrival times of *Ps* (t_1), *PpPs* (t_2) and *PpSs* + *PsPs* (t_3), given a crustal thickness H, V_p/V_s ratio κ and average crustal V_p or V_s. For our stacking an average crustal P-wave velocity of 6.5 km/s has been assumed from a previous refraction study in the Seychelles (Davies and Francis, 1964) and all phases are weighted equally. We calculate errors using two methods. First we use a bootstrapping technique (Efron and Tibshirani, 1991) where we randomly sample all the receiver functions n times, where n is the number of receiver functions estimated for each station (individual receiver functions can be included more than once) and perform the stacking technique. We repeat this 10,000 times and the standard deviation of these 10,000 estimates gives our 95% confidence interval. In some cases where we have few data, this technique may not be valid. However, we include this for all stations as it gives an indication of the stability of the result. The other estimate of error comes from the uncertainty in our assumed average crustal P-wave velocity. We test this by investigating the sensitivity of the results to a change in average crustal velocity of ± 0.2 km s^{-1}. Throughout this paper we use the larger of these errors.

5. Results

The results show considerable variability in Moho depth and V_P/V_S between islands in the Seychelles (Fig. 2, Table 1). The RFs can be split into four main groups based on location and RF characteristics, Mahé (MSEY, MHDLB, MHSPS, MHPLB, MMLPS), Praslin (ARDPS, CRSPS, FLCPS and PRTLB), Silhouette (NRDPS and SLHLB) and outer islands (DNSPB, DSRPS, PLTPB, ALPLB and CTVPS). Results for the individual islands are summarised in the following sections.

5.1. Mahé

Results from the H–κ stacking method on Mahé are well resolved with the permanent station MSEY and MHDLB being particularly well constrained (Fig. 2). Results are also consistent across the island giving a Moho depth between 28 and 33 km and V_P/V_S between 1.70 and 1.82 (Table 1 and Fig. 3). This is consistent with previous estimates of crustal thickness from controlled source data (Davies and Francis, 1964; Collier et al., 2009). A stack of all the Mahé stations produces an average result for the island of 31 ± 1 km and a V_P/V_S of 1.81 ± 0.03.

The stations MHSPS and MMLPS have a clearly identifiable *Ps* arrival, but due to the lack of observable multiples the H–κ stacking technique cannot be performed. However, we can still estimate the depth to the Moho by assuming V_p/V_s ratios from the stack of all Mahé stations using

$$H = \frac{t_{Ps}}{\sqrt{\frac{1}{V_S^2} - p^2} - \sqrt{\frac{1}{V_P^2} - p^2}}. \tag{2}$$

Using a *Vp* velocity of 6.5 km s^{-1}, a κ of 1.81 and an incoming P-wave from an event at 65° epicentral distance ($p = 0.05853$), we estimate a depth to the Moho of 33 km (MHSPS) and 28 km (MMLPS).

The exceptional quality of data recorded at the permanent station MSEY has previously been used for forward modelling (Hammond et al., 2012). This shows that the broadening of the *Ps* arrival and later multiples requires a thin high velocity layer at the base of the crust (see Fig. 3 in Hammond et al., 2012). To further highlight the necessity of this layer, Fig. 4 shows a comparison of fit to these data with and without a thin layer at the base of the crust. It is evident that a thin, high velocity layer at the base of the crust beneath Mahé fits the broad nature of the multiples much better. Hammond et al. (2012) performed grid search inversions on these data and showed that a well constrained thin high velocity layer at the base of the crust is required to fit the data.

5.2. Praslin and surrounding islands

Stations on or close to Praslin Island have a typical crustal thickness of 39–42 km and a V_P/V_S of 1.71–1.81 (Fig. 2 and Table 1). The stacked result for all Praslin stations is a crustal thickness of 41 ± 3 and V_p/V_s of 1.71 ± 0.09. We use this result and Eq. (2) to estimate crustal thickness at Aride (ARDPS) and Felicite (FLCPS) where multiples cannot be identified well. These crustal thicknesses are considerably thicker than neighbouring Mahé Island,

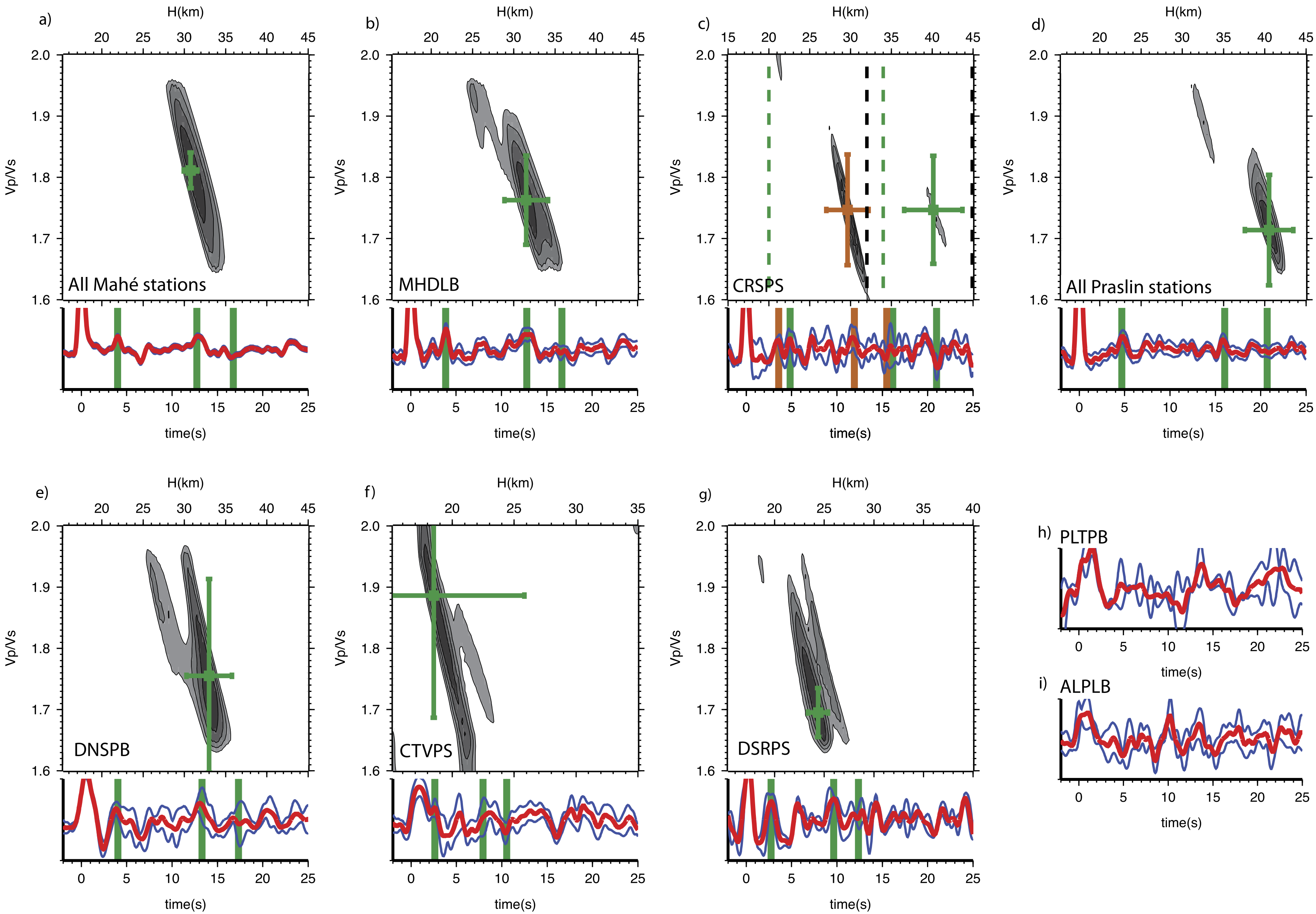

Fig. 2. The H–κ stacking results for a) all Mahé stations, b) MHDLB (Mahé), c) CRSPS (Curieuse), d) all Praslin stations, e) DNSPB (Denis), f) CTVPS (Coëtivy) and g) DSRPS (Desroche). Also shown are receiver function stacks for h) PLTPB (Île Platte) and i) ALPLB (Alphonse). The green cross shows the H–κ stacking result. Below each H–κ panel, the red receiver function shows the jackknife stacked receiver function and the surrounding blue receiver functions are the 95% confidence intervals. The green lines on the receiver function plots show the expected *Ps*, *PpPs* and *PsPs*–*PpSs* arrival times for the H–κ stacking result. The orange cross and lines shown in c) show a second solution for station CRSPS. The dashed lines in c) show the limited grid search used to isolate these two results. No obvious *Ps* time related to the Moho can be identified at PLTPB (h) or ALPLB (i). (For interpretation of the references to color in this figure legend, the reader is referred to the web version of this article.)

Table 1
Summary of crustal properties derived from H–κ stacking.

Station	Island	Latitude (°)	Longitude (°)	Crustal thickness (km)	V_P/V_S	NRF
Mahé Island						
MHDLB	Mahé	−4.63	55.43	32 ± 3	1.76 ± 0.07	17
MHPLB	Mahé	−4.79	55.53	33 ± 7	1.70 ± 0.24	4
MHSPS[a]	Mahé	−4.64	55.38	33	1.81	2
MMLPS[a]	Mamelle	−4.48	55.54	28	1.81	3
MSEY	–	−4.67	55.48	31 ± 1	1.82 ± 0.04	89
All stations	–	–	–	31 ± 1	1.81 ± 0.03	112
Praslin and satellite islands						
ARDPS[a]	Aride	−4.21	55.67	39	1.72	2
CRSPS (1)	Curieuse	−4.28	55.73	30 ± 3	1.75 ± 0.09	6
CRSPS (2)	Curieuse	−4.28	55.73	40 ± 4	1.75 ± 0.09	6
FLCPS[a]	Félicité	−4.32	55.87	42	1.72	6
PRTLB	Praslin	−4.30	55.71	39 ± 9	1.81 ± 0.12	12
All stations	–	–	–	41 ± 3	1.71 ± 0.09	24
Volcanic islands (Silhouette & Île du Nord)						
SLHLB	Silhouette	−4.49	55.25	33 ± 6	1.85 ± 0.13	6
NRDPS[a]	Île du Nord	−4.40	55.25	32	1.85	1
All stations	–	–	–	33 ± 5	1.85 ± 0.11	7
Coral atoll islands						
DNSPB	Denis	−3.81	55.67	33 ± 3	1.76 ± 0.16	4
ALPLB	Alphonse	−7.01	52.73	–	–	4
PLTPB	Île Platte	−5.86	55.38	–	–	2
DSRPS[b]	Desroche	−5.68	53.68	24 ± 1	1.69 ± 0.04	2
CTVPS	Coëtivy	−7.14	56.27	19 ± 7	1.89 ± 0.2	7

[a] κ taken from island stacks.
[b] No bootstrap error due to lack of receiver function data. NRF = number of receiver functions.

located just 50 km away (Fig. 3). However, on some stations a second, earlier peak can be identified on the receiver functions. This is best expressed on the island of Curieuse (CRSPS), just north of Praslin. Here the H–κ technique identifies two *Ps* arrivals and their multiples (Fig. 2). The first has a crustal thickness of 30 ± 3 km with V_p/V_s of 1.75 ± 0.09 and the second has a crustal thickness of 40 ± 4 km and a V_p/V_s of 1.75 ± 0.09. The shallower conversion is at a similar depth as the crustal thickness beneath Mahé. We propose that the deeper conversion is from the base of the thin high velocity layer identified beneath Mahé (Hammond et al., 2012), but with a thickness close to 10 km beneath Praslin. This is also consistent with results from the controlled source seismic data that show an underplated region beneath the northern Seychelles margin (Collier et al., 2009).

5.3. Silhouette

H–κ stacking of RFs at Silhouette (including one receiver function from neighbouring Île Du Nord) shows a crustal thickness of 33 ± 5, similar to Mahé, but the V_p/V_s is higher at 1.85 ± 0.11 (Fig. 2).

5.4. Outer islands

One station to the north of the main islands on Denis (DNSPB) has a crustal thickness of 33 ± 3 km and a V_p/V_s of 1.76 ± 0.16 (Fig. 2). This is consistent with controlled source results across the northern margin of the plateau (Collier et al., 2009).

To the south of the granitic islands a more complex picture is evident. Two stations are located on the Amirante Ridge on the islands of Desroche (DSRPS) and Alphonse (ALPLB). H–κ stacking estimates crust of 24 ± 1 km thick with a V_p/V_s of 1.69 ± 0.04 at Desroche, although this result is based on only 2 receiver functions. The station on Alphonse (ALPLB), has no clear *Ps* arrival and, is dominated by many peaks in the first 2 s (Fig. 2). This suggests that many shallow discontinuities may be present, and is very similar to the types of signals seen on receiver functions estimated for oceanic crust (Leahy and Park, 2005). Interestingly, the receiver function at Desroche shows little evidence of reverberations from shallow discontinuities (Fig. 2g) suggesting that the crust beneath this station is simple, similar to that seen beneath the topographic plateau.

Two other stations south of the Seychelles Plateau show similar results to Alphonse. This is particularly true for station Île Platte (PLTPB), where much energy in the first 2 s is followed by no clear *Ps* signal, similar to stations above oceanic crust (Leahy and Park, 2005) (Fig. 2). Alternatively, this characteristic signal could be due to a thick volcanic sequence above continental crust, a hypothesis supported by thick sequences of volcanics (> 900 m) encountered by a commercial drill hole at Constant Bank (Coakley, 1997) (Fig. 1). Receiver functions from the station on Coëtivy (CTVPS) also show signs of reverberations from shallow discontinuities, but it does give a reasonable H–κ stacking result with a crustal thickness of 19 ± 7 and V_p/V_s of 1.89 ± 0.2. However, it is unclear if this is indeed due to a primary conversion, or simply a multiple associated with the shallow discontinuities producing the signal in the first 2 s (Fig. 2).

6. Gravity modelling

To better constrain the nature of the crust around the Seychelles, particular the southernmost islands, we model historic gravity data (Fig. 5). We model the effect of a 2-D body of arbitrary shape, composed of constant density layers using a line-integral method (Bott, 1965). This assumes that the amount of 3-D structure is small, and the structure at the end of the profile extends to infinity.

The available gravity database provides a number of ship track profiles for modelling (Fig. 5). The chosen tracks are approximately orthogonal to the regional gravity field and also have simultaneously collected bathymetry data for inclusion in the models. The

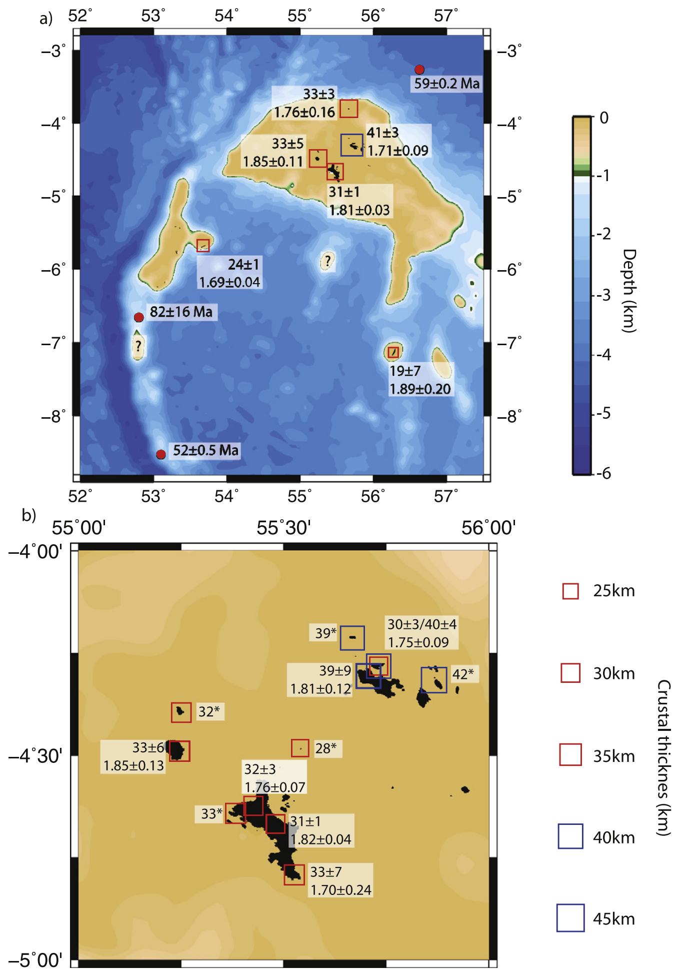

Fig. 3. Map showing crustal thickness and V_P/V_S across the Seychelles. Also shown are ages of volcanic rocks in the region (Fisher et al., 1968; Collier et al., 2008; Stephens et al., 2009).

aim of the modelling is to fit the $\sim$50–200 km wavelength gravity signals due to crustal scale features, and smaller wavelength features due to shallow structure (e.g., sedimentary basins) are ignored.

The velocity and density of the continental crust and mantle (layers 6–8) are taken from the receiver function inversions for Mahé (Hammond et al., 2012). The velocities for the oceanic crust (layers 3–5) are taken from global averages (Mooney et al., 1998), and the densities are calculated assuming empirical velocity (V_P; $\mathrm{km\,s^{-1}}$)–density (ρ; $\mathrm{g\,cm^{-3}}$) relationship for oceanic crust (Carlson and Herrick, 1990) and mantle rocks (Birch, 1961). Table 2 shows the velocities and densities used in the gravity modelling. A thin layer of sediment (layer 2) is placed between the water column (layer 1) and the top of the oceanic crust (layer 3). This has a typical sediment velocity of 2.1 $\mathrm{km\,s^{-1}}$ (Lowrie, 1997), and a density of 1.8 $\mathrm{g\,cm^{-3}}$ (Reynolds, 1997). For profile 2 the sediment thickness is constrained from the seismic reflection profiles shown in Mart (1988).

6.1. North margin

Fig. 5b shows the modelled gravity results from the northern Seychelles margin. Grey vertical bars show the receiver function estimates of depths to major discontinuities at stations closest to the gravity profiles. Profile 1 shows a narrow transition from oceanic to continental crust. A Moho depth of 33 ± 3 km is estimated from H–κ stacking beneath Denis on the northern edge of the Seychelles Plateau, and this agrees with the observed gravity. Seaward of this station the model has an abrupt transition from continental crust to oceanic crust, as seen in the controlled source data (Collier et al., 2009). Profile 1 also samples close to Curieuse (CRSPS) and the underplated layer seen in the receiver functions at this station fits the gravity well. The profile ends just before Mahé, however a model where the underplated layer thins towards Mahé is consistent with the gravity data. Tests on the sensitivity of the gravity models show that a model with thicker lower crust ($\rho = 2.82\ \mathrm{kg\,m^{-3}}$), but no lower crustal underplated layer ($\rho = 2.94\ \mathrm{kg\,m^{-3}}$) can fit the gravity data as well. However, this requires thicker crust than that imaged with the receiver functions, and also does not fit the controlled source seismic data, which requires this lower crustal layer.

Table 2
Seismic velocities and densities assumed for the gravity models. See text for details of relationships used for conversions from velocity to density.

V_P ($\mathrm{km\,s^{-1}}$)	ρ ($\mathrm{kg\,m^{-3}}$)	
1.54	1030	Sea Water
2.10	1800	Sediment
5.00	2410	Upper Oceanic Crust
6.00	2610	Middle Oceanic Crust
7.10	3040	Lower Oceanic Crust
6.00	2650	Continental Upper Crust
6.70	2820	Continental Lower Crust
7.10	2940	Lower Crustal Intruded Material
7.50	3080	Mantle

6.2. Southern margin

Gravity across the Amirante Ridge has been studied previously by Miles (1982). He found that a mass deficiency to the north–east of the ridge is necessary to fit the free-air anomaly. This is modelled as a small region of crustal shortening, which he suggests may have been the result of shallow subduction. We suggest an alternative model where the mass deficiency required by the gravity data can be explained by a region of continental crust $\sim$25 km thick. This matches the H–κ stacking result at Desroche (DSRPS) which lies on the eastern side of the Amirante Ridge (Fig. 5). As discussed previously, receiver functions from Alphonse, an island to the south, show many early arrivals. These are similar to those seen at other oceanic islands (Leahy and Park, 2005), where oceanic crustal thicknesses were estimated to be between 10 and 15 km, but sediments and volcanics overlying continental crust could also be the cause of the receiver function energy.

Receiver functions at Île Platte (PLTPB) and Coëtivy (CTVPS) are similar to those seen at Alphonse. Without better constraints from receiver functions it is not possible to determine a unique gravity model so the nature of the crust beneath this part of the Mascarene Basin remains unclear.

7. Discussion

7.1. Structure of the Seychelles Plateau

Evidence provided by receiver functions supports the idea that the Seychelles consists of a sliver of continental crust, with Moho depths beneath the topographic plateau between 28 and 41 km. Our work shows that thick continental crust exists to the northernmost extent of the plateau. This implies a relatively sharp transition to oceanic crust at the edge of the topographic plateau, which is supported by recent controlled source work (Collier et al., 2009). Beneath the topographic plateau we show evidence for a thick layer at the base of the crust at Praslin, which thins towards Mahé. Based on its seismic velocity and position we interpret this

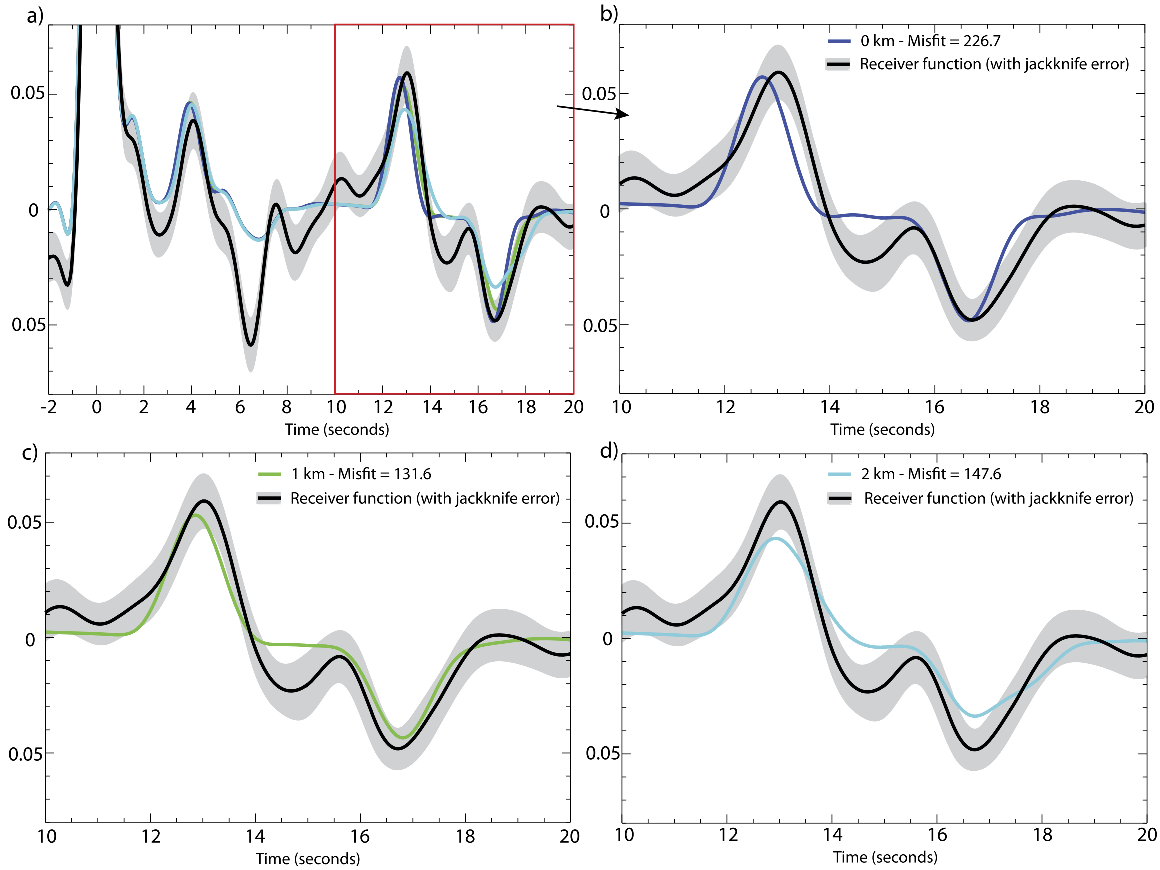

Fig. 4. Forward models for varying lower crustal layer thickness at station MSEY. a) The data-derived receiver function (black) with 95% confidence jackknife error bounds (grey). Also shown are synthetics based on the crustal model of Hammond et al. (2012) with varying lower crustal layer thickness (blue = 0 km, green = 1 km, cyan = 2 km). b)–d) show the multiples only (red box in a)) for the 3 different models. Misfit values are calculated using $\chi^2 = \sum_{i=1}^{N}(\frac{d_i - s_i}{\sigma_i})^2$ where d_i are the data-derived receiver function values, s_i are the synthetic receiver function values, σ_i are the jackknife estimated 2σ errors and N is the number of samples. Note that a thin layer 1–2 km thick at the base of the crust fits the broad multiples better than no layer e) shows the velocity models used to generate the synthetic RFs. (For interpretation of the references to color in this figure legend, the reader is referred to the web version of this article.)

layer as lower crustal intrusions of mafic material. The most likely explanation for the origin of this material is that it is plume-related. The Seychelles have been influenced by two large plume events, the Marion plume, which has been suggested to initiate rifting between the Madagascar and Seychelles/India (Storey et al., 1995) and the Deccan–Reunion plume, which was instrumental in the later breaking apart of India and the Seychelles (Müller et al., 2001) (Fig. 6). The earliest volcanism found on Madagascar associated with the Marion plume are ∼ 90 Ma (Storey et al., 1995; Torsvik et al., 1998) and similar age basalts are found in southwest India (Pande et al., 2001; Kumar et al., 2001), showing its influence may have affected our study area. Current plate reconstructions place our study area closer to the starting Deccan–Reunion plume, and volcanics directly related to the Deccan are found on the Seychelles (Dickin et al., 1986; Suwa et al., 1994). Although it is not possible to unequivocally determine whether the proximity of either of these two plumes is directly linked to the emplacement of the mafic material beneath the Seychelles crust, the fact the receiver function results show it to thin to the south may suggest a Deccan influence. In support of this interpretation we note that a thicker but otherwise similar layer of lower crustal high velocities is seen beneath the Laxmi Ridge (Minshull et al., 2008) and beneath Deccan influenced India (Rao and Tewari, 2005). If this interpretation is correct, the disappearance of this layer southwards across the Seychelles block suggests the Seychelles overlay the edge of the plume head during Deccan Trap formation an inference consistent with numerical modelling of the break-up magmatism that followed (Armitage et al., 2010).

7.2. Origin of the Amirante Ridge

South of the Seychelles Plateau, one of the receiver functions, Desroche in the northern Amirantes, shows evidence of 24 km thick crust with a low V_P/V_S of 1.69 ± 0.04 indicative of continental crust (Christensen, 1996), a model consistent with the gravity data (Fig. 5). There has been much debate in the literature about the origin of the Amirantes, with mechanisms ranging from subduction (Miles, 1982; Masson, 1984; Mart, 1988; Damuth and Johnson, 1989; Mukhopadhyay et al., 2012): transpression along a strike-slip fault formed during the opening of the West Somali Basin prior to the separation of Madagascar–Seychelles–India (Plummer, 1996) to a bolide impact (Hartnady, 1986). Based on our receiver function results we propose that the northern Amirantes is a small block of continental material. The lateral extent of this block is unclear, and in particular whether it is indeed isolated from the main topographic plateau to the north. However, given the clear topographic saddle between the two (unlike the southerly extension of Constant Bank) it seems highly likely that it is. Receiver functions from this study cannot resolve the nature of the crust in the southern Amirantes, however the interpretation of a significant change in crustal structure between the northern and central Amirantes is suggested by changes in both the along-strike gravity and magnetic fields. The northern Amirantes have a weak gravity anomaly to the west and a weak magnetic field of differing signs compared to the central Amirantes that have a strong negative, −120 mGal, anomaly to the west (the

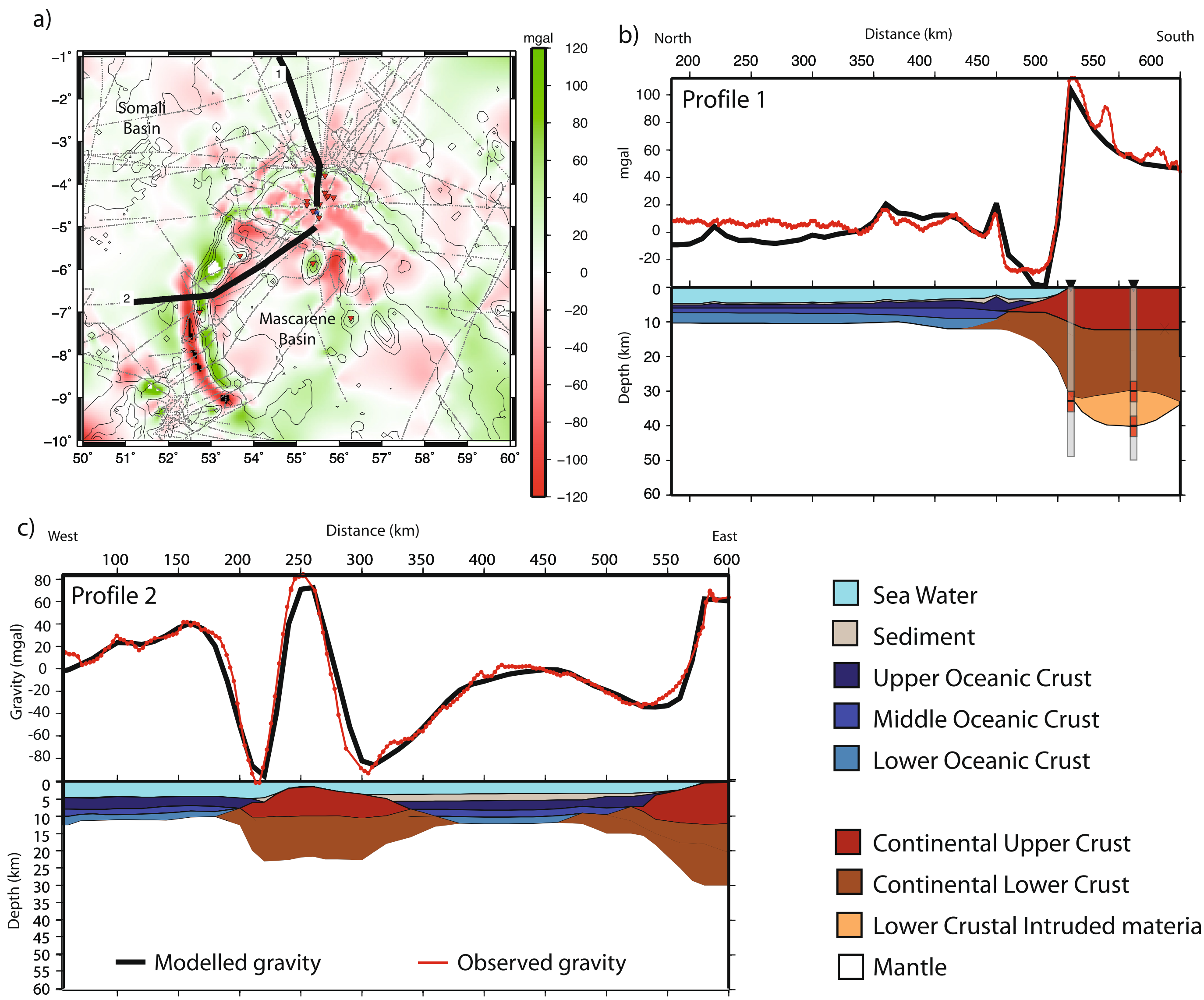

Fig. 5. a) The free-air gravity anomaly computed from all regional seaboard gravity data, along with bathymetry contours (Smith and Sandwell, 1997). Dashed and solid lines show the seaboard gravity profiles with solid lines showing those modelled in this study. b) and c) Gravity modelling for the two profiles shown in a). Each figure shows observed and modelled gravity in the top plot, with the best-fitting model shown below. Grey vertical bars, and black lines show approximate locations of receiver functions and estimated depths to major discontinuities. The red box on the grey bars shows Moho depth errors. (For interpretation of the references to color in this figure legend, the reader is referred to the web version of this article.)

Amirante Trough) and a strong positive, 200 nT magnetic field (see Fig. 3 in Tararin and Lelikov, 2000).

The difficulty in interpreting the nature of the Amirantes region has been both a paucity of data and also the inconsistency of the data. Here we suggest that the recognition of fundamental differences in structure between the northern and central/southern parts can resolve this. For example, only two dated samples exist for the region a sample from 6°40′ S giving an age of 82 ± 16 Ma (Fisher et al., 1968) and the other one recovered at 8°32′ S giving a much younger age of 51.4 ± 0.9 Ma (Stephens et al., 2009) (Fig. 3). Such a discrepancy is difficult to reconcile with a single mechanism for the entire Amirante complex. However, within the context of our new interpretation we interpret the former as Marion-plume associated magmatism preserved on the northern Amirantes continental block (similar to the interpretation of volcanics found in the Amoco drillholes on the southwest tip of the Seychelles Plateau; Plummer and Belle, 1995) whereas the later is due to whatever mechanism formed the central/southern Amirantes. The rotational opening of the Mascarene Basin may well have caused compression in the north–west region of the newly forming Mascarene Basin, and it has been suggested that this is the cause of the Amirante ridge/trough complex. Our new data do not rule this out as a possible explanation for the formation of the central and southern Amirantes. More comprehensive geophysical/geochemical studies of the Amirantes are required to address this.

7.3. *New insights into the opening of the Indian Ocean*

Fig. 6 summarises our new results within the context of previous work on the tectonic evolution of the western Indian Ocean. The cartoon updates that of Plummer and Belle (1995), to include the recognition of additional continental blocks, notably northern Amirantes (this study), Laxmi Ridge (Minshull et al., 2008) and Mauritia (Torsvik et al., 2013). The recognition of continental crust beneath the northern Amirantes suggests that as the Seychelles–Madagascar–India broke apart more blocks of continental material

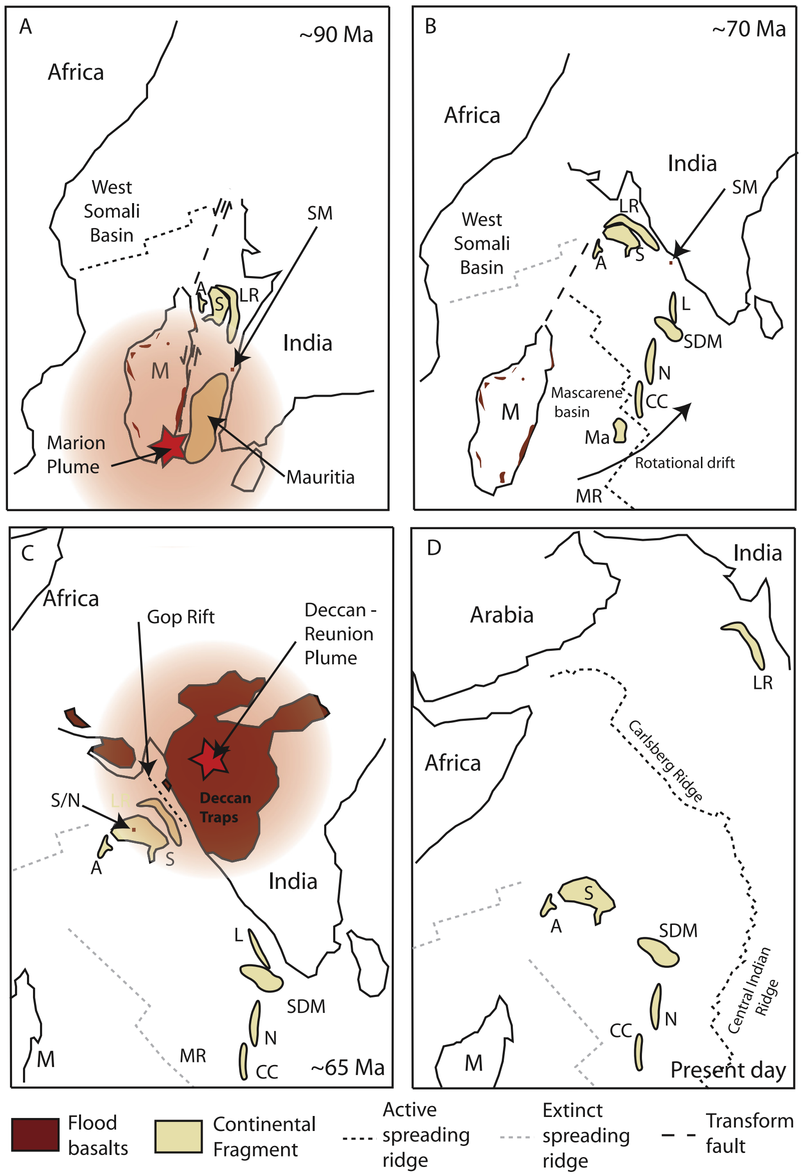

Fig. 6. Cartoon showing the formation of the Indian Ocean. A) The eruption of the Marion plume initiates rifting between Greater India (India, Seychelles, Mauritia and other fragments) and Madagascar. Red shaded region shows igneous outcrops associated with the flood basalt event (Storey et al., 1995; Torsvik et al., 1998; Pande et al., 2001; Kumar et al., 2001). B) The creation of the Mascarene Basin causing the rotational drift of Seychelles/India. The Amirantes (this study) and other microcontinents (Torsvik et al., 2013) are formed in the Mascarene Basin due to a series of rift jumps. C) The Seychelles/India at the Cretaceous/Tertiary boundary, the approximate time when spreading stopped in the Mascarene Basin and started at the Gop Rift/Carlsberg Ridge isolating the Laxmi Ridge (Minshull et al., 2008) and Seychelles (Collier et al., 2009). Red shaded region shows the Deccan traps large igneous province. F) The present day geographical arrangement. A = Amirante Ridge, CC = Cargados-Carajos, L = Laccadive Ridge, LR = Laxmi Ridge, M = Madagascar, Ma = Mauritius, MR = Mascarene Ridge, N = Nazareth, S = Seychelles, SDM = Saya de Malha, SID = South Indian Dykes, SM = St Mary's Islands, S/N = Silhouette and Île du Nord. Adapted from Plummer and Belle (1995). (For interpretation of the references to color in this figure legend, the reader is referred to the web version of this article.)

may have been isolated than previously thought. This possibility is consistent with the idea that rotational opening of the Mascarene Basin was likely accommodated by a series of rift jumps, isolating small slivers of continental crust in the Mascarene Basin (Torsvik et al., 2013) (Fig. 6). It is unfortunate that seafloor-spreading anomalies are lacking in the northern Mascarene Basin to better define the pattern of breakup (Bernard and Munschy, 2000). In contrast the rifting that severed the Seychelles from India, likely linked with the Deccan–Reunion plume (Collier et al., 2008) from 65 Ma is well constrained by supporting seafloor-spreading anomalies. Rifting occurred initially along the Gop Rift, between the Laxmi Ridge and India and subsequently along the Carlsberg Ridge which finally isolated the Laxmi Ridge and Seychelles continental fragments (Minshull et al., 2008; Collier et al., 2009).

7.4. The role of mantle plumes in microcontinent formation

Our interpretation adds to the growing body of evidence that mantle plumes can initiate ridge jumps and the formation of microcontinents. Other examples where this association has been reported include Jan Mayen microcontinent (Müller et al., 2001), East Tasman Sea (Gaina et al., 2003) and Kerguelan Plateau (Bénard et al., 2010). Continental lithosphere is inherently weaker than oceanic lithosphere (Steckler and ten Brink, 1986) meaning it is easier to rift than unrifted oceanic lithosphere. However, an additional mechanism is required to facilitate a new rift forming at the expense of an active spreading ridge. The presence of melt has been shown to significantly weaken continental lithosphere further (Buck, 2004) meaning the initiation of a plume head below continental lithosphere may be enough to weaken the lithosphere to a degree that allows a ridge jump to occur (Müller et al., 2001). Other mechanisms such as subduction processes (McCrory et al., 2009) or changes in far field forces (Peron-Pinvidic et al., 2012) may be responsible for microcontinent formation, but again in these cases a mechanism to significantly weaken the lithosphere is needed and the presence of melt is often invoked. Significant strike-slip faulting was present in the region during Madagascar/Seychelles breakup (Fig. 6) and so mechanisms such as shear heating (Minakov et al., 2013) may have had a role. However, the presence of the Marion plume in the southern Mascarene Basin during rifting between Madagascar and Seychelles/India suggests that this was likely to have influenced rift jumps and the formation of microcontinents in the southern Mascarene Basin (Torsvik et al., 2013), thus it is possible that this was responsible for isolating the Amirante continental block.

8. Conclusions

Receiver function analysis confirms the presence of continental material beneath the Seychelles topographic plateau. Additionally, the presence of a layer of lower crustal intrusions beneath the Seychelles, thinning to the south, shows that the Seychelles lay at the edge of the Deccan plume during the emplacement of the Deccan Traps although a Marion Plume influence cannot be ruled out. Indeed, the presence of multiple plume events so close may be a factor in explaining why the lithosphere beneath the Seychelles is so unusual (Hammond et al., 2012). This supports the idea that mantle plumes have instigated rifting between Madagascar, Seychelles and India (Storey et al., 1995; Torsvik et al., 1998; Müller et al., 2001; Gaina et al., 2003; Collier et al., 2009; Armitage et al., 2010, 2011; Hammond et al., 2012).

South of the topographic plateau we identify an unrecognised sliver of continental material beneath the northern Amirante Ridge, adding to the recent observation of small continental slivers within the Indian Ocean (e.g., Laxmi Ridge (Minshull et al., 2008), Mauritia (Torsvik et al., 2013)), and in other regions of continental breakup in flood basalt affected regions (e.g., Tasman Sea, Australia (Müller et al., 2001; Gaina et al., 2003), Norwegian–Greenland Sea (Gudlaugsson et al., 1988), Afar, Ethiopia/Eritrea/Djibouti (Eagles et al., 2002; Hammond et al., 2011)). These observations suggest that as continental breakup occurs in the presence of mantle plumes, it may be common that many small fragments of continental material become isolated within oceanic crust.

Acknowledgements

We would like to thank all those involved in the fieldwork, especially Tim Minshull, Bob Whitmarsh, James Wookey, Graham Stuart, Nick Teanby, Trond Ryberg, Ali Schulze and Jen Caddick. Considerable logistic support came from many people, companies and government agencies in the Seychelles. In particular we would like to thank Seychelles National Oil Company (Patrick Joseph and Patrick Samson), Seychelles Centre Marine Research Technology (Evariste Michel and Jude Bijoux), Island Development Committee (Justin Moustache), Marine Parks Authority, Ministry of Tourism (Eddie Belle), Ministry of Environment (Rolph Poyet and Victorin Laboudallon), Gondwana Granite (Selwyn Gendron), Seychelles Marketing Board and Seychelles Island Foundation, and the managers/owners of the following Islands: Bird, Denis, Aride, Cousine, Felicite, La Digue, Silhouette, Île du Nord, Coëtivy, Île Platte, Desroche and Alphonse. The instrument pool of GeoForschungsZentrum Potsdam is thanked for providing seismic stations. Funding was provided by NERC, grant NER/A/S/2000/01390, the Royal Society, grant RSRG 24044, and the GeoForschungsZentrum Potsdam. James Hammond is supported by NERC Fellowship NE/I020342/1.

References

Abers, G.A., Hu, X., Sykes, L.R., 1995. Source scaling of earthquakes in the Shumagin region, Alaska: Time-domain inversions of regional waveforms. Geophys. J. Int. 123, 41–58.

Ammon, C.J., 1991. The isolation of receiver effects from teleseismic P waveforms. Bull. Seismol. Soc. Am. 81, 2504–2510.

Ammon, C.J., Randall, G.E., Zandt, G., 1990. On the nonuniqueness of receiver function inversions. J. Geophys. Res. 95, 15303–15318.

Armitage, J.J., Collier, J.S., Minshull, T.A., 2010. The importance of rift history for volcanic margin formation. Nature 465, 913–917.

Armitage, J.J., Collier, J.S., Minshull, T.A., Henstock, T.J., 2011. Thin oceanic crust and flood basalts: India–Seychelles breakup. Geochem. Geophys. Geosyst. 12, Q0AB07, http://dx.doi.org/10.1029/2010GC003316.

Ashwal, L.D., Demaiffe, D., Torsvik, T.H., 2002. Petrogenesis of Neoproterozoic granitoids and related rocks from the Seychelles: the case for an Andean arc origin. J. Petrol. 43, 45–83.

Bénard, F., Callot, J.P., Vially, R., Schmitz, J., Roest, W., Patriat, M., Loubrieu, B., 2010. The Kerguelen plateau: Records from a long-living/composite microcontinent. Mar. Petroleum Geol. 27, 633–649.

Bernard, A., Munschy, M., 2000. Le bassin des Mascareignes et le bassin de Laxmi (océan Indien occidental) se sont-ils formés à l'axe d'un même centre d'expansion? Earth Planet. Sci. 330, 777–783.

Birch, F., 1961. Velocity of compressional waves in rocks to 10 kilobars. Part 2. J. Geophys. Res. 66, 2199–2224.

Bott, M.H.P., 1965. The upper mantle beneath Iceland. Geophys. J. R. Astron. Soc. 9, 275–277.

Buck, W.R., 2004. Consequences of asthenospheric variability on continental rifting. In: Karner, G.D., Taylor, B.N., Droscoll, W., Kohlstedt, D.L. (Eds.), Rheology and Deformation of the Lithosphere at Continental Margins. Columbia Univ. Press, New York, pp. 1–30.

Carlson, R.L., Christensen, N.I., Moore, R.P., 1980. Anomalous crustal structures in ocean basins: Continental fragments and oceanic plateaus. Earth Planet. Sci. Lett. 51, 171–180.

Carlson, R.L., Herrick, C.N., 1990. Densities and porosities in the oceanic crust and their variations with depth and age. J. Geophys. Res. 95, 9153–9170.

Christensen, N.I., 1996. Poisson's ratio and crustal seismology. J. Geophys. Res. 101, 3139–3156.

Coakley, G.J., 1997. The mineral industry of islands of Comoros, Mauritius, Reunion and Seychelles. Technical report. USGS, Reston, Virginia.

Collier, J.S., Minshull, T.A., Hammond, J.O.S., Whitmarsh, R.B., Kendall, J., Sansom, V., Lane, C.I., Rümpker, G., 2009. Factors influencing magmatism during continental breakup: New insights from a wide-angle seismic experiment across the conjugate Seychelles–Indian margins. J. Geophys. Res. 114, B03101.

Collier, J.S., Sansom, V., Ishizuk, O., Taylor, R., Minshull, T.A., Whitmarsh, R.B., 2008. Age of Seychelles–India break-up. Earth Planet. Sci. Lett. 272, 264–277.

Damuth, J.E., Johnson, D.A., 1989. Morphology, sediments and structure of the Amirant Trench, Western Indian-Ocean – implications for trench origin. Mar. Petroleum Geol. 6, 232–242.

Darwin, C., 1839. Journal of Researches into the Geology and Natural History of the Various Countries Visited by the HMS Beagle. Penguin Books, London.

Davies, D., Francis, T.J.G., 1964. The crustal structure of the Seychelles bank. Deep-Sea Res. 11, 921–927.

Dickin, A.P., Fallick, A.E., Halliday, A.N., MacIntyre, R.M., Stephens, W.E., 1986. An isotopic and geochronological investigation of the younger igneous rocks of the Seychelles microcontinent. Earth Planet. Sci. Lett. 81, 46–56.

Eagles, G., Gloaguen, R., Ebinger, C., 2002. Kinematics of the Danakil microplate. Earth Planet. Sci. Lett. 203, 607–620.

Efron, B., Tibshirani, R., 1991. Statistical data analysis in the computer age. Science 253, 390.

Fisher, R.L., Engel, C.G., Hilde, T.W.C., 1968. Basalts dredged in the Amirante Ridge, western Indian Ocean. Deep-Sea Res. 15, 521–534.

Francis, T.J.G., Davies, D., Hill, M.N., 1966. Crustal structure between Kenya and the Seychelles. Philos. Trans. R. Soc. Lond. A 259, 240–261.

Francis, T.J.G., Shor, G.G., 1966. Seismic refraction measurements in the Northwest Indian Ocean. J. Geophys. Res. 71, 427–449.

Franks, L., Sloan, D., Sloan, M., Matchette-Downes, C.J., 2006. An oil prone frontier basin. GeoExpro 10, 40–44.

Gaina, C., Müller, R.D., Brown, B., Ishihara, T., 2003. Microcontinent formation around Australia. In: Hillis, R., Müller, R.D. (Eds.), The Evolution and Dynamics of the Australian Plate. In: Geological Society of America Special Papers, vol. 372, pp. 405–416, and Geological Society of Australia Special Publications, vol. 22.

Ganerod, M., Torsvik, T.H., Hinsbergen, D.J.J.V., Gaina, C., Corfu, F., Werner, S., Owen-Smith, T.M., Ashwal, L.D., Webb, S.J., Hendriks, B.W.H., 2011. Palaeoposition of the Seychelles microcontinent in relation to the Deccan Traps and the Plume Generation Zone in Late Cretaceous–Early Palaeogene time. In: Hinsbergen, D.J.J.V., Butter, S.J.H., Torsvik, T.H., Gaina, C., Webb, S.J. (Eds.), The Formation and Evolution of Africa: A Synopsis of 3.8 Ga of Earth History. In: Special Publications, vol. 357. Geological Society, London, UK, pp. 229–252.

Gaskell, T.F., Hill, M.N., Swallow, J.C., 1958. Seismic measurements made by H.M.S. Chalenger in the Atlantic, Pacific and Indian Oceans and in the Mediterranean Sea, 1950–53. Philos. Trans. R. Soc. Lond. A 251, 23–83.
Gudlaugsson, S.T., Gunnarsson, K., Sand, M., Skogseid, J., 1988. Tectonic and volcanic events at the Jan Mayan Ridge microcontinent. Geol. Soc. London 39, 85–93.
Gurrola, H., Baker, G.E., Minster, J.B., 1995. Simultaneous time-domain deconvolution with application to the computation of receiver functions. Geophys. J. Int. 120, 537–543.
Hammond, J.O.S., Collier, J.S., Kendall, J., Helffrich, G., Rumpker, G., 2012. Plume scar in the mantle lithosphere beneath the Seychelles revealed by seismic imaging. Earth Planet. Sci. Lett. 355–356, 20–31.
Hammond, J.O.S., Kendall, J., Rümpker, G., Wookey, J., Teanby, N., Joseph, P., Ryberg, T., Stuart, G., 2005. Upper mantle anisotropy beneath the Seychelles microcontinent. J. Geophys. Res. 110, B11401.
Hammond, J.O.S., Kendall, J., Stuart, G.W., Keir, D., Ebinger, C.J., Ayele, A., Belachew, M., 2011. The nature of the crust beneath the Afar triple junction: Evidence from receiver functions. Geochem. Geophys. Geosyst. 12, Q12004, http://dx.doi.org/10.1029/2011GC003738.
Hartnady, C.J.H., 1986. Amirante basin, western Indian Ocean: Possible impact site of the cretaceous/tertiary extinction bolide? Geology 14, 423–426.
Helffrich, G., 2006. Extended-time multi-taper frequency domain cross-correlation receiver function estimation. Bull. Seismol. Soc. Am. 96, 344–347.
Kumar, A., Pande, K., Venkatesan, T.R., Rao, Y.J., 2001. The Karnataka Late Cretaceous Dykes as products of the Marion Hot Spot at the Madagascar–India breakup event: Evidence from ^{40}Ar–^{39}Ar geochronology and geochemistry. Geophys. Res. Lett. 28, 2715–2718.
Langston, C.A., 1979. Structure under Mount Rainier, Washington, inferred from teleseismic body waves. J. Geophys. Res. 84, 4749–4762.
Leahy, G.M., Park, J., 2005. Hunting for oceanic island Moho. Geophys. J. Int. 160, 1020–1026.
Ligorria, J.P., Ammon, C.J., 1999. Iterative deconvolution and receiver-function estimation. Bull. Seismol. Soc. Am. 89, 1395–1400.
Lowrie, W., 1997. Fundamentals of Geophysics. Cambridge University Press.
Mart, Y., 1988. The tectonic setting of the Seychelles, Mascarene and Amirante plateaus in the Western Equitorial Indian Ocean. Mar. Geol. 79, 261–274.
Masson, D.G., 1984. Evolution of the Mascarene Basin, western Indian Ocean and the significance of the Amirante arc. Mar. Geophys. Res. 6, 365–382.
Matthews, D.H., Davies, D., 1966. Geophysical studies of the Seychelles bank. Proc. R. Soc. Lond. 259, 227–239.
McCrory, P.A., Wilson, D.S., Stanley, R.G., 2009. Continuing evolution of the Pacific–Juan de Fuca–North America slab window system – A trench–ridge-transform example from the Pacific Rim. Tectonophysics 464, 30–42.
Miles, P.R., 1982. Gravity models of the Amirante Arc, western Indian Ocean. Earth Planet. Sci. Lett. 61, 127–135.
Minakov, A.N., Podladchikov, Y.Y., Faleide, J.I., Huismans, R.S., 2013. Rifting assisted by shear heating and formation of the Lomonosov Ridge. Earth Planet. Sci. Lett. 373, 31–40.
Minshull, T.A., Lane, C.I., Collier, J.S., Whitmarsh, R.B., 2008. The relationship between rifting and magmatism in the northeastern Arabian Sea. Nat. Geosci. 1, 463–467.
Mooney, W.D., Laske, G., Masters, G., 1998. Crust 5.1: a global crustal model at 5×5 degrees. J. Geophys. Res. 103, 727–747.
Mukhopadhyay, R., Karisiddaiah, S.M., Ghosh, A.K., 2012. Geodynamics of the Amirante ridge and trench complex, western Indian Ocean. Int. Geol. Rev. 54, 81–92.
Müller, R.D., Gaina, C., Roest, W.R., Hansen, D.L., 2001. A recipe for microcontinent formation. Geology 29, 203–206.
Nur, A., Ben-Avraham, Z., 1982. Oceanic plateaus, the fragmentation of continents, and mountain building. J. Geophys. Res. 87, 3644–3661.
Oldenburg, D.W., 1981. A comprehensive solution to the linear deconvolution problem. Geophys. J. R. Astron. Soc. 65, 331–357.
Owens, T.J., Zandt, G., Taylor, S.R., 1984. Seismic evidence for an ancient rift beneath the Cumberland Plateau, Tennessee; a detailed analysis of broadband teleseismic P waveforms. J. Geophys. Res. 89, 7783–7795.
Pande, K., Sheth, H.C., Bhutani, R., 2001. ^{40}Ar–^{39}Ar of the St. Mary's Islands volcanics, southern India: record of India–Madagascar break-up on the Indian subcontinent. Earth Planet. Sci. Lett. 193, 39–46.
Park, J., Levin, V., 2000. Receiver functions from multiple-taper spectral correlation estimates. Bull. Seismol. Soc. Am. 90, 1507–1520.
Peron-Pinvidic, G., Gernigon, L., Gaina, C., Ball, P., 2012. Insights from the Jan Mayen system in the Norwegian–Greenland sea–I. Mapping of a microcontinent. Geophys. J. Int. 191, 385–412.
Plummer, P.S., 1996. The Amirante ridge/trough complex: response to rotational transform rift/drift between Seychelles and Madagascar. Terra Nova 8, 34–47.
Plummer, P.S., Belle, E.R., 1995. Mesozoic tectono-stratigraphic evolution of the Seychelles microcontinent. Sediment. Geol. 96, 73–91.
Rao, S.P., Tewari, H.C., 2005. The seismic structure of the Saurashtra crust in northwest India and its relationship with the Reunion Plume. Geophys. J. Int. 160, 319–331.
Reynolds, J.M., 1997. An Introduction to Applied and Environmental Geophysics. Wiley.
Shor, G.G., Pollard, D.D., 1963. Seismic investigations of Seychelles and Saya de Malha Banks, Northwest Indian Ocean. Science 142, 48–49.
Smith, W.H.F., Sandwell, D.T., 1997. Global sea floor topography from satellite altimetry and ship depth soundings. Science 277, 1956–1962.
Steckler, M.S., ten Brink, U.S., 1986. Lithospheric strength variations as a control on new plate boundaries: examples from the northern Red Sea region. Earth Planet. Sci. Lett. 79, 120–132.
Stephens, W., Storey, M., Donaldson, C., Ellam, R., Lelikov, E., Tararin, G., Garbe-Schoenberg, C., 2009. Age and origin of the Amirante ridge–trench structure, western Indian Ocean. In: AGU Fall Meeting Abstracts, p. 1885.
Storey, M., Mahoney, J., Saunders, A., Duncan, R., Kelley, S., Coffin, M., 1995. Timing of hot spot-related volcanism and the breakup of Madagascar and India. Science 267, 852–855.
Suwa, K., Tokieda, K., Hoshino, M., 1994. Palaeomagnetic and petrological reconstruction of the Seychelles. Precambrian Res. 69, 281–292.
Tararin, I.A., Lelikov, E.P., 2000. Amirante island arc in the Indian Ocean: Data on the initial island-arc magmatism. Petrology 8, 53–65.
Torsvik, T., Amundsen, H., Hartz, E.H., Corfu, F., Kusznir, N., Gaina, C., Doubrovine, P.V., Steinberger, B., Ashwal, L.D., Jamtveit, B., 2013. A Precambrian microcontinent in the Indian Ocean. Nat. Geosci. 6, 223–227, http://dx.doi.org/10.1038/ngeo1736.
Torsvik, T.H., Tucker, R.D., Ashwal, L.D., Eide, E.A., Rakotosolofo, N.A., Wit, M.J., 1998. Late Cretaceous magmatism in Madagascar; paleomagnetic evidence for a stationary Marion hotspot. Earth Planet. Sci. Lett. 164, 221–232.
Tucker, R.D., Ashwal, L.D., Torsvik, T.H., 2001. U–Pb geochronology of Seychelles granitoids: a Neoproterozoic continental arc fragment. Earth Planet. Sci. Lett. 187, 27–38.
Wegener, A., 1924. The Origin of Continents and Oceans. Methuen, New York.
Weis, D., Deutsch, S., 1984. Nd and Pb isotope evidence from the Seychelles granites and their xenoliths – Mantle origin with slight upper-crust interaction for alkaline anorogenic complexes. Isot. Geosci. 2, 13–35.
Zandt, G., Ammon, C.J., 1995. Continental crust composition constrained by measurements of crustal Poisson's ratio. Nature 374, 152–154.
Zhu, L., Kanamori, H., 2000. Moho depth variation in southern California from teleseismic receiver functions. J. Geophys. Res. 105, 2969–2980.